**The Report Committee for John Paul Bergstrom**
**Certifies that this is the approved version of the following report:**

# High-Speed High-Power Permanent Magnet Machine Parameters, Qualities, and Considerations

**APPROVED BY**
**SUPERVISING COMMITTEE:**

**Supervisor:**

Mircea D. Driga

Andrea Alù

# High-Speed High-Power Permanent Magnet Machine Parameters, Qualities, and Considerations

**by**

**John Paul Bergstrom, BSEE**

**Report**

Presented to the Faculty of the Graduate School of

The University of Texas at Austin

in Partial Fulfillment

of the Requirements

for the Degree of

**Master of Science in Engineering**

**The University of Texas at Austin**

**May 2013**

## Acknowledgements

I would like to acknowledge my advisor, Professor Driga, for his guidance through my Master's. Dr. Driga's extensive background and knowledge in electromagnetics and machines gave me great appreciation of this complex and extensive field. As I return to industry employment, I am vary grateful for the knowledge and experiences I have obtained will at the University of Texas.

# Abstract

## High-Speed High-Power Permanent Magnet Machine Parameters, Qualities, and Considerations

John Paul Bergstrom, MSE

The University of Texas at Austin, 2013

Supervisor: Mircea D. Driga

Permanent magnet machines have become an attractive topology for several applications due to their high power density and brushless qualities as compared to conventional wound field machines or squirrel cage machines. The presences of permanent magnets provide distinct advantages, but at the same time unique behaviors that must be accounted for. Recent work has developed permanent magnet machines for high-power and high-speed applications such as may be found in the petro-chemical industry, naval ships, and energy storage systems.

# Table of Contents

# List of Tables

# List of Figures

# Chapter 1

# Introduction

Permanent magnet (PM) machines provide distinct advantages over other machine designs such as induction machines or wound-field machines. Use of the permanent magnets eliminates the need for brushes or winding of a wound-field machine and thus simplifies the rotor design. Also, the synchronous nature of the permanent magnet machine allows for more accurate speed control than a squirrel cage induction machine. While PM machines have found extensive use in small servo drives such as for hard drives which need very tight high-speed control but relatively low power, use of permanent magnets on an industrial scale machines has been more limited.

High-speed is generally considered to be anything above 3600 rpm. This is also the synchronous speed of a two pole machine operating off a 60 Hz line. Several industrial devices such as compressors and vacuum pumps operate at much higher speeds than 3600 rpm and have traditionally been operated by machines such as solid rotor induction machines. As a generator, the machine could be directly coupled to the shaft of a gas-turbine which tend to operate in the range of 15 000 rpm. This would eliminate the need for gear reduction in the system, improving efficiency, and reducing system complexity and volume. As machine speed and power increases, the mechanical aspects require extra attention. Instead of just providing mechanical structure and magnetic flux paths, the tensile strength of the material must be considered to prevent catastrophic damage. The centrifugal forces produced would destroy some rotor designs.

In this report, some of the key aspects of PM machines will be discussed. A particular focus will be given towards requirements to produce high-speed and high-power PM machines as well discussion of current work and designs reported in literature.

# Chapter 2

# Permanent Magnet Materials

The first modern permanent magnets were developed in the 1930's and referred to as Alnico magnets due to their primary composition of aluminum, nickel, and cobalt. These types of magnets can produce very high magnetic field strength and possess higher temperature capabilities than other permanent magnets. However, they are very susceptible to demagnetization and therefore rarely used for electric machinery.

## 2.1 MODERN MATERIALS

"Hard" ferrite magnets, often referred to as ceramics, were developed in the 1950's by combining elements such as strontium or barium with iron oxides. "Soft" ferrite materials can be made through the use of manganese-zinc or nickel-zinc. The hard or soft attribute describes the magnetic coercivity. Hard refers to high coercivity and resistance to demagnetization such as is needed for a high quality permanent magnet. Soft ferrites would be used for components like inductors and transformers because their internal magnetic fields can be easily reversed with relatively low loss of energy. Higher coercivity of ferrite magnets made them much more suitable for use in electric machinery than Alnico. They are still susceptible to demagnetization by high air gap flux densities produced by a short circuited generator or similar event. High resistivity in ferrite magnets helps limit losses due to eddy currents. Also, being inexpensive, they are widely used as common household magnets or as the classic horseshoe and bar magnets.

Rare-earth magnets became commercially available in the 1970's for samarium-cobalt (Sm-Co) and followed by higher energy neodymium-iron-boron (Nd-Fe-B) in the 1980's. Both of these materials exhibit high remanence characteristics, but, more importantly, they have high coercivities. This makes them much more resistant to

demagnetization than Alnico or ferrite. Sm-Co tends to be fairly high cost, but is much more thermally stable than Nd-Fe-B which also suffers from corrosion issues. In recent years, the cost for both materials has increased greatly with rising demand in China who is also the world's primary source. Table 1 below gives a summary of various magnetic characteristics for the discussed materials.

Table 1: Parameters of Several Magnetic Materials [1]

| Property | Units | Alnico | Anisotropic Ferrite | Sintered Sm-Co | Sintered Nd-Fe-B |
|---|---|---|---|---|---|
| Remanence $B_r$ | T | 0.6 – 1.35 | 0.35 – 0.43 | 0.7 – 1.05 | 1.0 – 1.3 |
| Intrinsic Coercivity $H_{ci}$ | kA/m | 40 – 130 | 180 – 400 | 800 – 1500 | 800 – 1900 |
| Recoil Permeability $\mu_{rec}$ | | 1.9 – 7 | 1.05 – 1.15 | 1.02 – 1.07 | 1.04 – 1.1 |
| $(BH)_{max}$ | $kJ/m^3$ | 20 – 100 | 24 – 36 | 140 – 220 | 180 – 320 |
| Magnetizing Force | kA/m | 200 – 600 | 600 – 1700 | 1600 – 4000 | 2000 – 3000 |
| Resistivity | μΩcm | 47 | $>10^4$ | 86 | 150 |
| Thermal Expansion | $10^{-6}$/°C | 11.3 | 13 | 9 | 3.4 |
| $B_r$ Temperature coefficient | %/°C | -0.01 to -0.02 | -0.2 | -0.045 to -0.05 | -0.08 to -0.15 |
| $H_{ci}$ temperature coefficient | %/°C | -0.02 | 0.2 – 0.4 | -0.2 to -0.25 | -0.5 to -0.9 |
| Max. working temperature | °C | 500 – 550 | 250 | 250 – 350 | 80 – 220 |
| Curie temperature | °C | 850 | 450 | 700 – 800 | 310 – 350 |
| Density | $kg/m^3$ | 7300 | 4900 | 8200 | 7400 |

The table shows clearly some of the trade-offs between the different materials that were mentioned earlier. While Alnico can produce the highest flux density of 1.35 tesla, comparable flux densities by the rare-earth's come with much better coercivity. Even then, the higher energy neodymium comes with the lowest working and Curie temperature of any of the materials discussed. Also, while ferrite magnets can be safely demagnetized by heating past the Curie temperature and then remagnetized, the other materials will suffer metallurgical changes before reaching Curie temperatures and irreversibly damage the magnet [1].

### 2.2 DEMAGNETIZATION

The B-H relationship of a typical ceramic magnet is shown in Figure 1. The classic flat topped magnetization curve of a permanent magnet is indicated by $B_i$. The $B_m$ demagnetization curve shows the cumulative effect of an external field applied to the magnet with the magnet's permeability as governed by Equation 2.1. As opposing H-field is increased, the effective B-field in the magnet will eventually reach zero at coercivity $H_c$. If the entire second quadrant characteristic remains a straight line, the magnet is termed a high-grade permanent magnet. If a magnet has a non-linear characteristic in the second quadrant, it is referred to as a low-grade permanent magnet. Figure 2 shows typical demagnetization curves of the four magnet materials discussed earlier with Alnico being the only low-grade material.

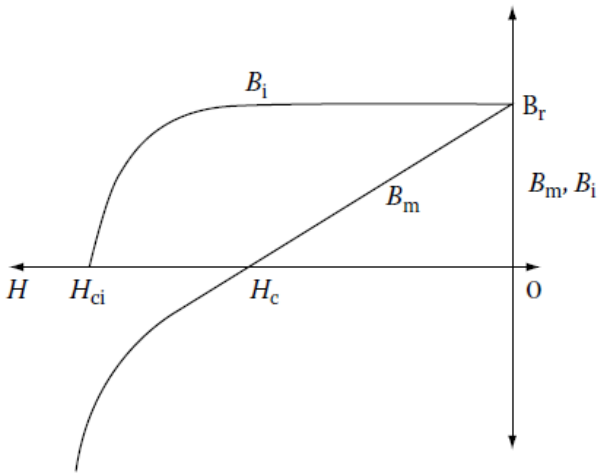


Figure 1: Typical Ceramic Magnet Flux Densities [2]

$$B_m = B_r + \mu_0 \mu_{rm} H \tag{2.1}$$

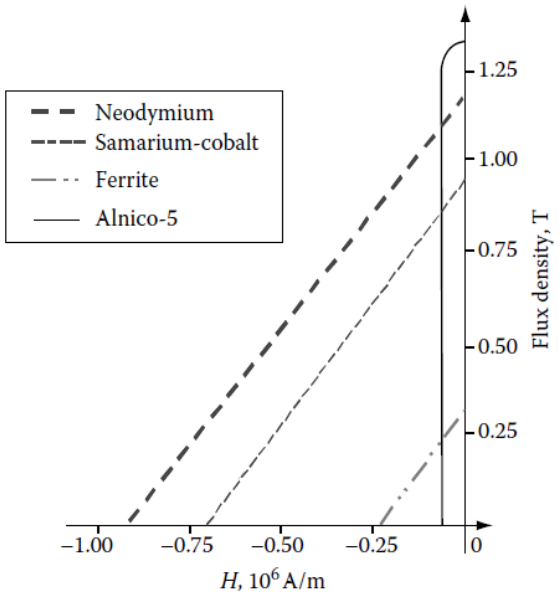


Figure 2: Demagnetization Curves of Common Magnetic Materials [2]

Krishnan, where the previous figures were obtained, goes into further detail on determining the operating point of the magnet which is also dependant on the magnetic path. As such, the operating point will always be less than Br due to the required air gap excitation. Figure 3 shows more detail related to the load lines as well as the recoil line of a low grade magnet. Forcing a magnet below its knee will cause it to recoil back to a lower $B_r$ than before. This is one of the primary concerns of using permanent magnets in a machine. Even partial demagnetization of the magnets will reduce the machine's output capabilities.

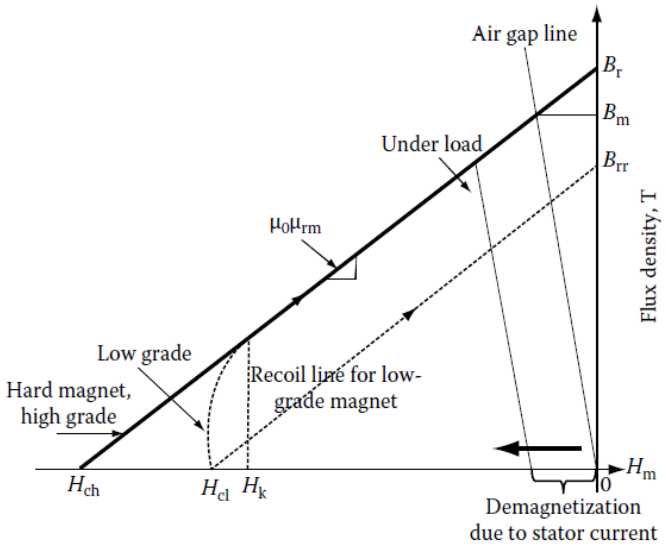


Figure 3: Operating Point of Magnets [2]

# Chapter 3

# Machine Topology

Similar to how wound field machines can have significant variation in the pole winding placement, poles comprised of permanent magnets can be formed in many ways. Conceptually, a ring shaped magnet may be the simplest shape. It could be slid over a steel laminated rotor and magnetized in any direction. Individual magnets, on the other hand, can take any shape.

## 3.1 Magnetic Pole Construction

Particularly with large machines, a ring magnet may not be economical or even possible due to machining and magnetization requirements. Figure 4 below shows some common individual magnet shapes that could be used to form machine poles. While the rectangular and radial shaped magnets nominally produce uniform fields, the breadloaf shape will produce a non-uniform field due to its variation in thickness. Rectangular shaped magnets are more commonly found in Interior Permanent Magnet (IPM) machines with multiple magnets used for each pole to facilitate a higher flux weakening region of operation [2]. They would not be suitable for surface mount machines due to the importance of maintaining a consistent air gap.

After the shape of the magnet is chosen, the direction of magnetization will have significant effects on the air gap flux density. As shown in Figure 5, a radial magnet could be magnetized in the radial direction normal to the curvature or parallel to a given axis. The effect on air gap flux density can be seen in Figure 6 where radial magnets in a two pole and many slotted machine have been simulated with radial and parallel magnetization by Krishnan.

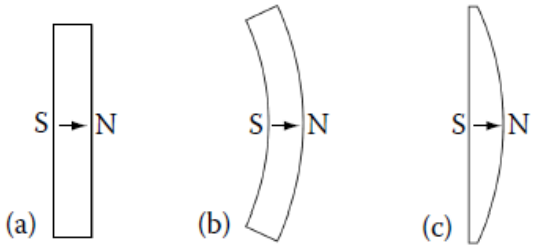


Figure 4: Magnetic Shapes: (a) Rectangular; (b) Radial; (c) Breadloaf [2]

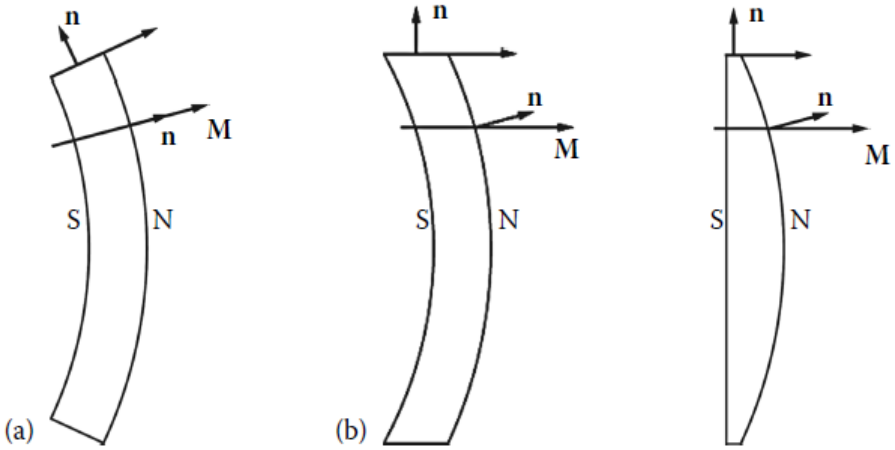


Figure 5: Magnetization of Magnets: (a) Radial; (b) Parallel [2]

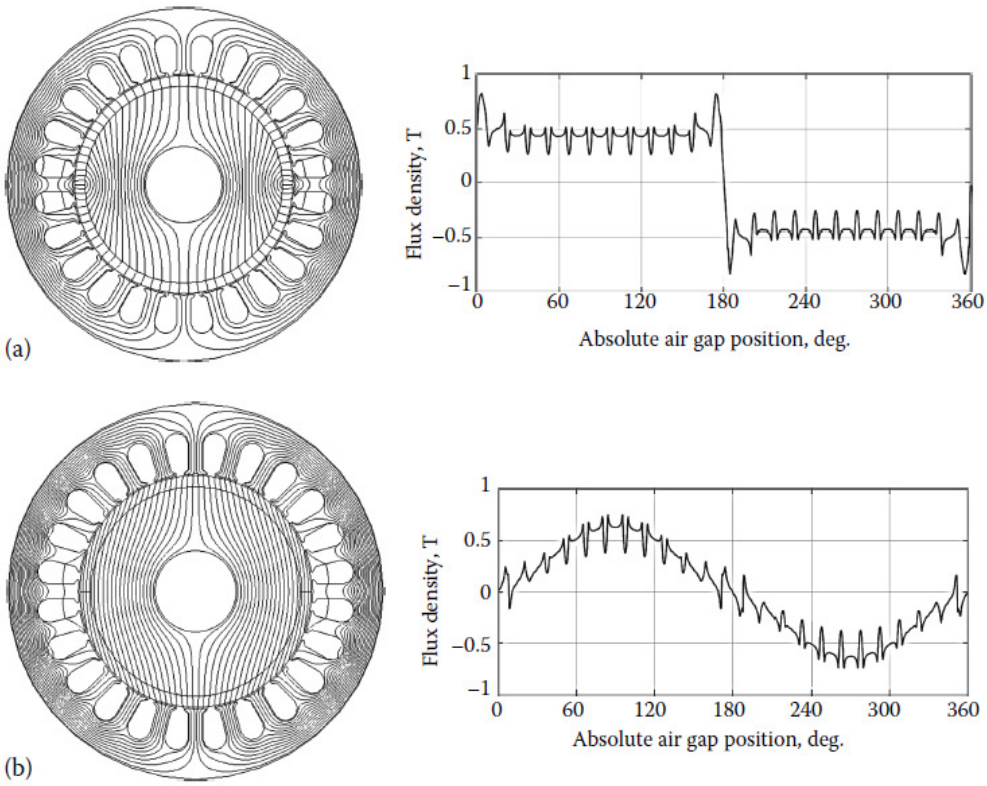


Figure 6: Flux and flux density versus rotor position for radially and parallel magnetized machines: (a) Radially Magnetized Machine; (b) Parallel Magnetized Machine [2]

With radial magnetization, a square wave distribution of magnetic flux would ideally be created with the transition happening where the pole changes from north to south. With parallel magnetization, a sinusoidal distribution is created. The high frequency content is created by the spatial harmonics of the stator slots. Which distribution is desired would depend on the application. For instance, in a generator application, the sinusoid may be more useful. Less filtering would be required to produce a clean sinusoid assuming the machine was spinning at the right frequency. In high speed applications, generating or motoring, the square distribution may be better due to limitation of the switch electronics on the terminals of the motor.

In conventional machines, operating off a normal 60Hz AC line, inverters and rectifiers can be controlled to produce 6 or 12 pulse waveform to reduce the harmonics going into or coming out of the machine. In high power applications, IGBT's are most commonly used due to the voltage and power conditions. However, for large machines, IGBT's may only be capable of switching at 1-2 kHz due to high switching losses and current tailing. In the case of a 3-phase machine rotating at 20 000 rpm, there is simply not enough time for a multi-pulse approach. The rotor will have physically rotated out of the spatial frame of the phase winding before a multi-step action can be employed.

### 3.2 SEVERAL TYPES OF PM MACHINES

Figure 7 shows examples of several interior-rotor PM machines topologies. Figure 7.a shows four magnets epoxied to a square rotor yoke with a multi-tooth punched stator surrounding it. The outside surface of the magnets would have to be ground after assembly for final dimensioning. Figure 7.b shows a bonded ring magnet which can be made from ferrite as well as rare-earth materials. The ring is less likely to fail due to rotational forces and skewed poles can be easily created to reduce cogging torques [1]. Figure 7.c uses sintered arc magnets with a retaining ring. Grinding would be required on both sides of the retaining ring as well as the outer magnet surfaces.

Figure 7.d shows a variation of a block magnet or arc magnet rotor. If the two magnets are alike, the motor is referred to as a consequent-pole machine. The second set of poles is effectively created in the soft ferrite extending from the rotor at 180 electrical degrees. If the two magnets are not alike, the machine is then a hybrid between a PM machine and a switched reluctance machine with high saliency. The design trades off the number of magnets for a machine with lower permeance.

Figure 7.e is a spoke-magnet or embedded magnet design. By magnetizing the magnet circumferentially, the effective poles are produced in the iron located between the magnets. With six or more poles, ferrite magnets in this configuration can produce flux densities comparable to surface-mounted rare-earth materials [1]. The rotor may be larger than an equivalent surface-mounted rare-earth and have larger inertia. However, in servo systems where low inertia is not required, the extra inertia can actually be beneficial in maintaining speed consistency.

The last example, Figure 7.f, is very similar to the first one except that the rotor core is round with arc magnets epoxied to its surface. Minimal grinding should be required unless a retaining can is required. Such a can is often needed in higher speed and power machines.

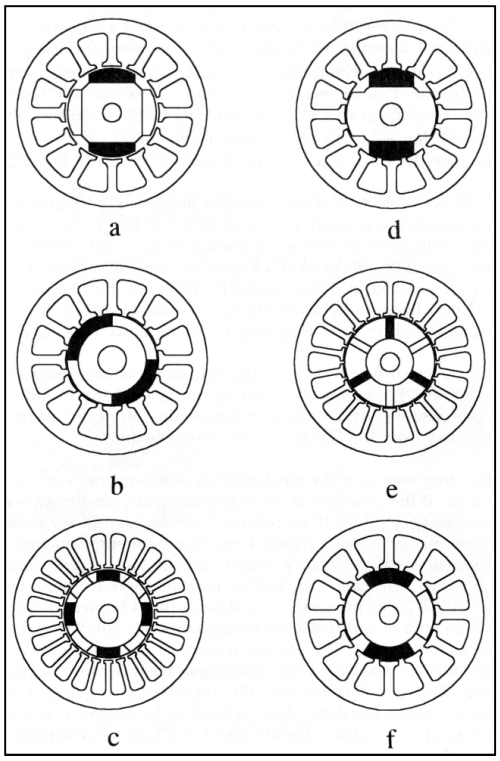


Figure 7: Examples of PM machine topologies [1]

# Chapter 4

## Flux Weakening

In many motors, certain types of speed control can be implemented by directly manipulating the air gap flux density. This is particularly evident in a DC machine with a shunt-excited field winding as displayed in Figure 8. As the terminal voltage, $V_t$ increases, so will the field and armature currents and motor speed until the armature current reaches its rated value. This occurs at the motor's base speed. The motor could then be run at higher speeds, but lower Torque, by decreasing the field current while the armature voltage and current remain constant. The relationship is shown through Equations 2-5.

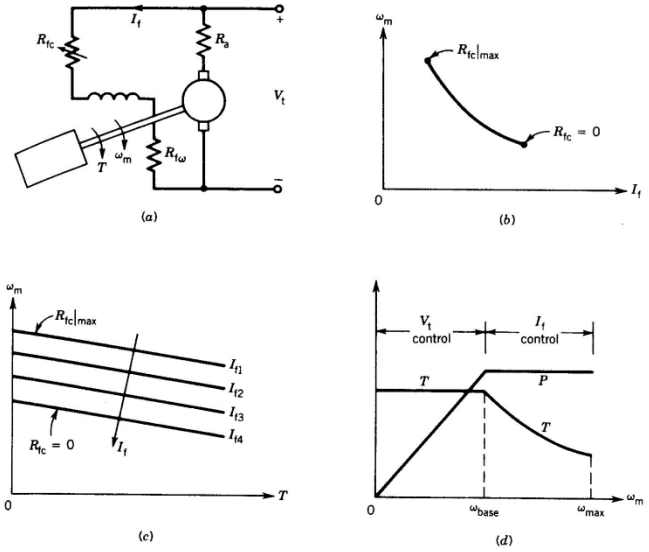


Figure 8: Flux Weakening Operation [3]

$$P = V_t I_a \tag{4.1}$$

$$\approx E_a I_a \tag{4.2}$$

$$T\omega_m = E_a I_a \tag{4.3}$$

$$T = \frac{E_a I_a}{\omega_m} \approx \frac{constant}{\omega_m} \tag{4.4}$$

Since the speed has an inverse relationship with the field current, as the field current decreases, the speed goes up. If the speed goes up, the torque must then reduce in order to maintain power balance in Equation 4.3. This type of control scheme is common for DC machine or wound-field induction machines where constant power operation is desired. Though, due to the inductance in the field coils, the response may be a bit slow [3]. However, with PM machines, the air gap flux density cannot be directly controlled. "Flux weakening" control must be accomplished indirectly.

As with other electrical machines, a PM machine can be described in the d-q reference frame as developed by Park [4]. For flux weakening operation, instead of directly reducing the air gap flux produced by the poles, which is not possible for a PM machine, negative d-axis current is injected into the windings such discussed by Sebastian and Slemon [5] and Morimoto [6]. A generalized method for developing smooth torque control under flux weakening of fault tolerant PM machines was introduce by Wang, Atallah, and Howe [7]. It was later shown by Sun, Wang, Jewell, and Howe [8] that this method was not sufficient and produced undesirable torque behavior under flux weakened fault conditions. An enhanced method was developed and tested where the weighting factor is adjusted in real time to produce much smooth torque response. Štumberger *et al.* [9] first presented the concept of using segmented poles with iron bridges between the magnets to increase the flux weakening effects for a given amount of negative d-axis current. This topology was also later discussed and tested by Dutta and Rahman [10] and shown to have very wide constant power speed range.

# Chapter 5

# Short-Circuit

There are numerous ways in which short circuit faults can be presented to an electric machine. Lines leading to the machine could be damaged. The power electronics operating the machine could fail. Insulation in the winding could breakdown. A foreign object could span two conductors. Typically, a short-circuit fault will result in higher than normal currents in the machine whose excess power is dissipated as heat in the windings or steel of the machine. The magnitude of the current is dependent on the impedances of the machine. When a generator suffers an external short-circuit, the current can be described by Equation 5.1 as given by Klontz [11].

$$i_a = \sqrt{2}E_{q1}\left[\underbrace{\frac{1}{X_d}}_{SS} + \underbrace{\left(\frac{1}{X_d'} - \frac{1}{X_d}\right)e^{-t/T_d'}}_{TRANSIENT} + \underbrace{\left(\frac{1}{X_d''} - \frac{1}{X_d'}\right)e^{-t/T_d''}}_{SUBTRANSIENT}\right]\cos(\omega t + \lambda) - \sqrt{2}E_{q1}e^{-t/T_a}\left[\frac{\cos(\lambda)}{x_m} + \frac{\cos(2\omega t + \lambda)}{x_n}\right] \tag{5.1}$$

This equation, or some form of it, is commonly found in machine theory and power systems books such as by Concordia [12], Adkins [13], and Glover [14]. The first bracketed terms are the AC terms dependent on machine impedances. The term $E_{q1}$ refers to the open circuit electromotive force. The $X_d$ term is the synchronous reactance of the machine which controls the steady state behavior. The $X_d$' term is the transient reactance which comes from the field winding in the case of wound-field generators. A Permanent Magnet Generator (PMG) has no field winding. So, this term and its associate time constants are undefined. The subtransient terms relates to the conductive components of the rotor such as the magnets, retaining sleeves, and shaft. Since the PMG has no field

winding, Klontz puts forth to set the transient reactance $X_d$' equal to the synchronous reactance $X_d$. This eliminates the transient term, but leaves the correct subtransient term. After the subtransient term decays, the current is still solely limited by the synchronous reactance. The λ term relates to the timing of the fault compared to the phase angle of the current at time equal to zero. The $x_m$ and $x_n$ terms related to pole saliency. The λ term appears again in the second set of terms as it produces a DC offset effect.

It is well established, that the DC offset can more than double the initial peak current during a short circuit [12], [13], [14], [15], [16]. Klontz also shows how with a PMG, the DC term could offset the AC completely to one side of the time axis making it completely positive or negative for several cycles. This is due to the subtransient reactance and time constant of a PMG being significantly smaller than the synchronous reactance and armature time constant. Klontz also gives a comparative table of parameters between a PMG and WFG which is displayed in Table 2.

Table 2: A comparison of PMG and WFG parameters [11]

| p.u. values except where stated; values may vary widely | | PMG | WFG |
|---|---|---|---|
| Xd | d-axis synchronous reactance | 0.45 | 1.20 |
| Xd' | d-axis transient reactance | -- | 0.35 |
| Xd'' | d-axis subtransient reactance | 0.13 | 0.25 |
| Xq | q-axis synchronous reactance | 0.45 | 0.90 |
| Xq' | q-axis transient reactance | -- | 0.35 |
| Xq'' | q-axis subtransient reactance | 0.13 | 0.28 |
| Td0' | d-axis open-circuit transient time-constant | -- | 6.0 s |
| Td' | d-axis short-circuit transient time-constant | -- | 1.4 s |
| Td0'' | d-axis open-circuit subtransient time-constant | 28 ms | 260 ms |
| Td'' | d-axis short-circuit subtransient time-constant | 8.0 ms | 160 ms |
| Tq'' | q-axis short-circuit subtransient time-constant | 8.0 ms | 160 ms |
| Ta | Armature time-constant | 15 ms | 91 ms |

Since permanent magnets have permeability similar to that of air, they can increase the effective air gap of the magnetic paths. This could result in increased

reluctance which would then decrease the inductance and reactance terms as is seen in Table 2 for PMG machines compared to a WFG machine.

Sun gives another consideration of short circuits in a PM machine [17]. Sun performed analysis and experiments on a five phase fault tolerant 250 kW PM motor. The motor is made fault tolerate by isolated all the inverters and supplies to each phase as well and designing the synchronous reactance's to be one per unit to limit current under short circuit. However, instead of a terminal short as mentioned before, Sun analyzes an inter-turn short between turns in the winding. These types of shorts are more likely to occur in the first few turns of the winding as incoming voltage wave fronts from the inverter produce large voltage gradients [17].

An extreme example of a large incident wave front would be a machine subjected to a lightning event. The voltage induced by a lightning strike distributes capacitively across each turn of the winding and the inductance of the winding has minimal effect initially [18]. Sun developed an analytical model, supported by FE analysis, to predict the short circuit current based on where in the winding a short occurred. Sun then experimentally showed that a short in the turns closer to the rotor will result in current significantly above rated. In Sun's experiment, steady state short-circuit currents reached 4-5 times rated current.

# Chapter 6

## High-Speed and High-Power

With advances in switching converters, the limiting factors for high-speed high-power electrical machine shifts towards the mechanical and thermal considerations. Gas turbines can easily be running at 20 000 rpm. Attaching an electrical machine directly to the turbine shaft eliminates gear boxes, mechanical losses, costs, as well as volume. The reliability is then increased, and if magnetic or gas bearing are used, the whole drive system can be oil free. High-speed machines also have applications in compressors, vacuum pumps, and flywheel energy storage. Arkkio [19] presents Figure 9 which gives and indicative spread of power and speed levels of numerous machines as found in IEEE Electronic library and the internet in general. The figure suggests that PM machines have the edge in regards to electromagnetic performance. However, induction machines have the benefit of lower material costs and optimized production costs due to their long history. While squirrel cage motors still have a very strong position for low and medium speed applications, PM machine have gained interest due to their better efficiency and power density.

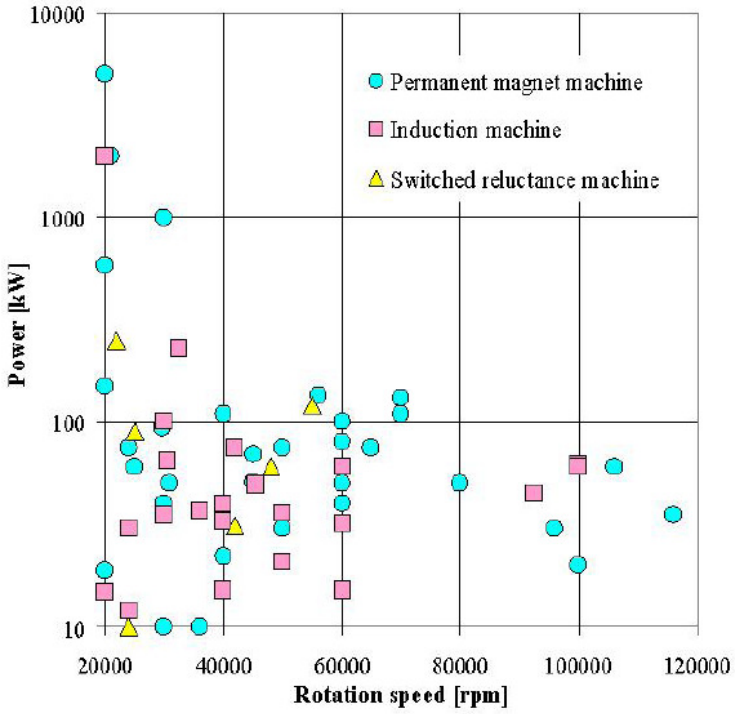


Figure 9: A sampling of power and speed ratings for different types of electrical machines [19]

### 6.1 Speed Limits Due to Material Properties

One of the most important considerations of high-speed machines is the rotor tip speed or surface speed of the outer diameter. Due to the fast rotations, rotor constructions used in lower speed machines are simply not robust enough to withstand the forces present at high speeds. Depending on the material, at a particular rotational velocity, the material will simply begin to fly apart. Solid rotor induction machines have been used for high speed machines due to their strength and rigidity [20]. Arkkio states that a solid steel rotor can withstand surface speeds of 400 m/s but suffer from large rotor losses and poor power factor [19]. Arkkio also suggests that above 300 m/s air resistance becomes a dominate loss component of the machine. Laminated rotors electrical steel is limited to speeds of about 200 m/s [19].

Arkkio also states that PM machines are limited to speeds of around 250 m/s, but does not give explicit reasoning. Likely, it is related to the ability retain the magnets to the rotor. At low speeds, the magnets can simply be bonded to the rotor or an embedded magnet design could be used. As speeds increase, these designs would provide insufficient radial stiffness in the rotor and mass containment as claimed by Bailey *et al.* [21].

Bailey *et al.* designed and tested an 8 MW PM machine at 15 000 rpm operating speed. A solid rotor core was used to provide stiffness, and a sleeve provided containment. Common sleeve materials include non-magnetic high strength alloys, pre-molded graphite or carbon composites, and wound-in-place carbon fiber or carbon-fiber composites [21]. Of these, carbon fiber provides the highest strength and minimal conduction paths for eddy currents induced by the air-gap flux. As a result, the actual limiting factor for magnet retention is the hoop stress of sleeve. Bailey states that while the tip speed of the designed machine falls below Arkkio's 250 m/s rule of thumb, the material limits would allow for speeds higher than that.

### 6.2 MACHINE LOSSES

Arkkio presents designs of PM and induction machines for three different power and speed levels: 540 kW at 30 000 rpm, 90 kW at 60 000 rpm, and 30 kW at 100 000 rpm. The PM machines were designed as four pole machines with magnets mounted on a solid steel core. An aluminum screen was used to reduce eddy current losses as also mentioned by Bailey. In addition, a carbon fiber sleeve was used for retention. The induction machines were solid rotor two-pole machines. The PM machines were chosen as four-pole to mitigate armature reaction, and the induction machines were chosen as two-pole to limit the size of the air gap [19]. A cross-section of both motors is shown in

Figures 10 and 11. FEM analysis was done to determine losses due to electromagnetics as well as friction. The results are shown in Figure 12.

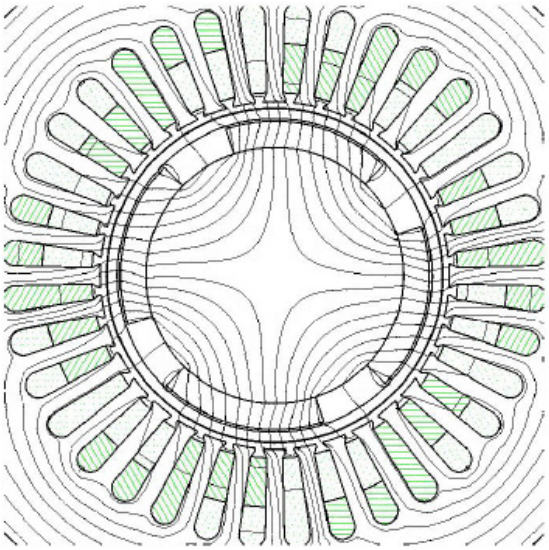

Figure 10: Finite Element cross-section of a segmented PM machine [19]

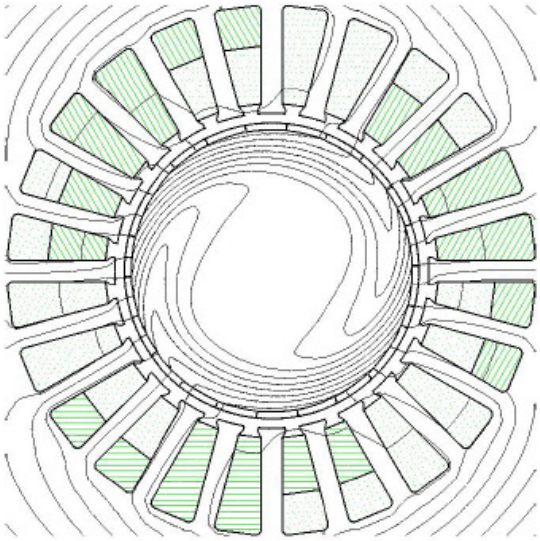

Figure 11: Finite element cross-section of solid rotor induction machine [19]

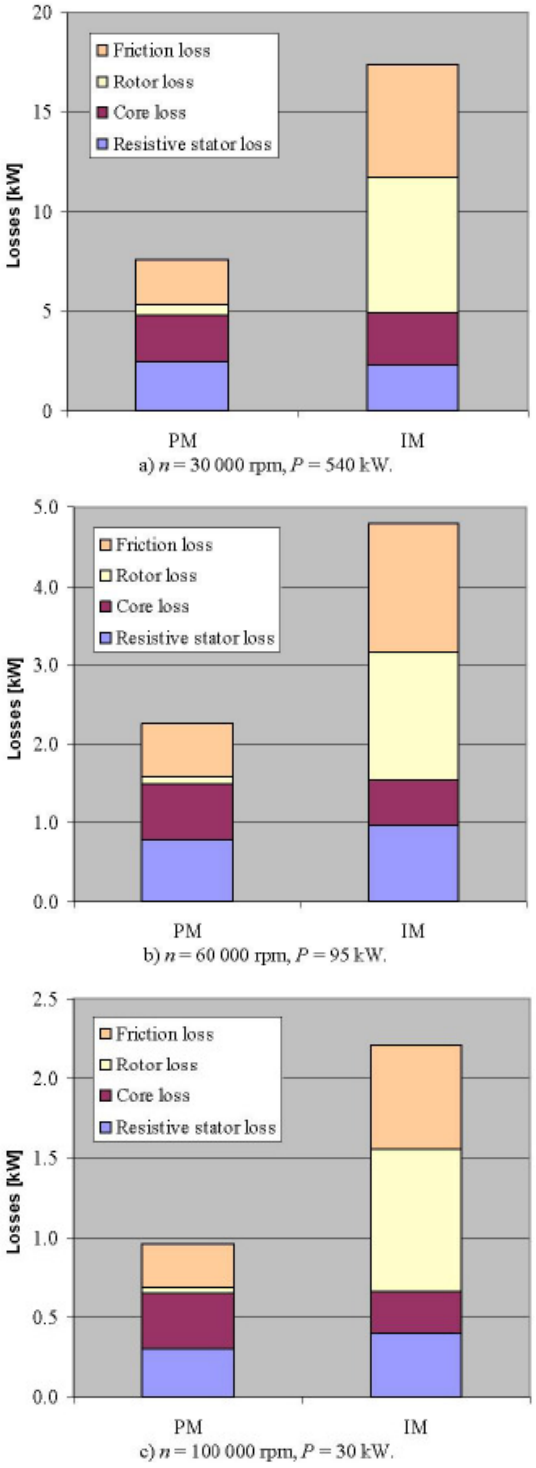


Figure 12: Segmented losses of three machine operating points using PM and IM machines [19]

In all three cases, the PM machine has half or less losses than the induction machine. The rotor losses, which are minor in the PM machine, are the dominate loss in the induction machine. The graphs show machine efficiencies of about 98% for the PM machine versus 96% for the induction machine.

### 6.3 TESTING OF 8 MW 15 000 RPM PM MACHINE

Bailey's machine was tested in generation mode being driven by a 3 MW gas turbine at 15 000 rpm [22]. Figure 13 shows the measured results of the test as well as predicted results of several models of the machine. Table 3 shows the loss segregation according to the models at 3 MW operation. Bailey discusses that the differences in the models produce 0.2-0.7% difference in machine efficiency from 3 MW to 8 MW operation [22]. As seen in Figure 13, the lumped parameter (LP) model agrees very well with the measured results. Differences between the LP and computation fluid dynamics (CFD) models may somewhat be accounted for by the LP model not handling the skin effects in the end turns properly. While this may seem to indicate errors in the loss segregation of the CFD model, its good correlation with predicted and measured temperatures which is very important for the expected temperature rise of various components and less so for the power conversion calculation [22].

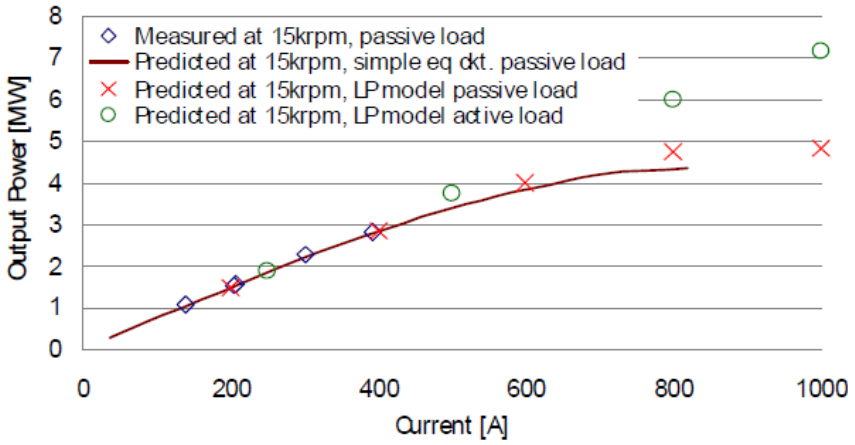


Figure 13: Predicted and measured results of Bailey PM machine [22]

Table 3: Segregated losses of Bailey PM machine [22]

| | Iron Loss [kW] | Slot Cu Loss [kW] | End-turn Cu Loss [kW] | Windage [kW] | Total loss [kW] |
|---|---|---|---|---|---|
| **CFD Model** | 33.60 | 21.2 | 1.77 | 17.80 | 74.37 |
| **FE Model** | 23.77 | 9.95 | 1.72 | n/a | n/a |
| **LP Model** | 24.46 | 1.91 | 1.71 | 20.0 | 48.08 |

Several other tests besides the 3 MW 15 0000 rpm operation were also performed. The FE model predicted an open circuit voltage of 4392 volts at 15 000 rpm with the measured result being 4378 volts, but, as Bailey mentions in [22], the open circuit voltage varies almost linearly with speed. The no-load open-circuit voltage was measured across the speed range and normalized for speed. The results are shown in Figure 14 and show consistent values.

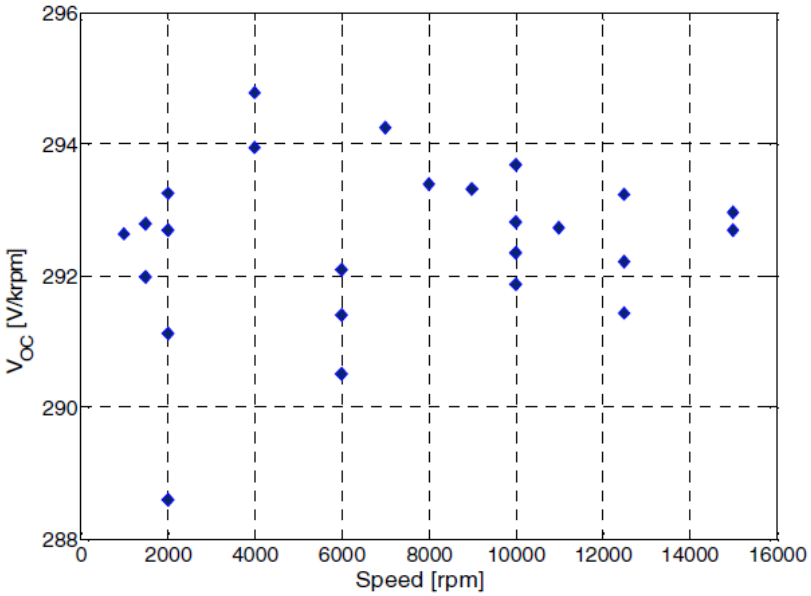


Figure 14: Open-circuit voltage normalize for rotor speed versus rotor speed [22]

Short-circuit testing was also performed. This is a critical test for a permanent magnet machine due to the concern about demagnetization. The machine was operated as a generator at a low speed of 2 000 rpm. Why this speed was chosen is not clear. However, since the reactances will nominally scale linearly with speed, the short-circuit current profiles should be similar. A typical result of the low-speed test is shown in Figure 15. This shows a steady-state current of about 1700 amps. This is very close already to what could be considered rated current of 1827 amps based on the 8 MW and 4378 volts parameters. The steady-state current is more an issue of localized heating rather than demagnetization. The greatest risk of demagnetization will come from the initial peak which, in this test, is about 3300 amps. Subsequent tests of the normalized open-circuit voltage for speed to be nearly unchanged indicating that the magnets were not damaged.

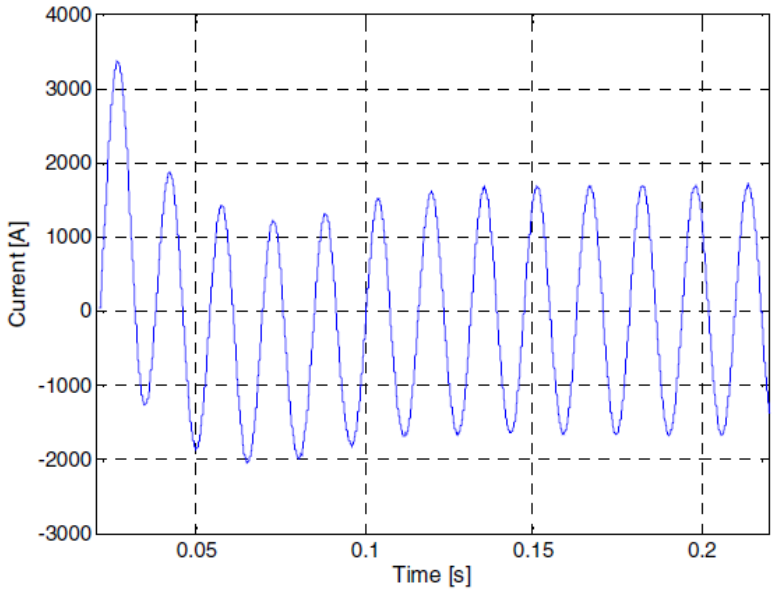


Figure 15: Typical short-circuit response of Bailey PM machine [22]

Through the short-circuit testing, the reactances of the machine were determined at the 2 000 rpm speed. With key assumptions regarding linearity supported via modeling and testing, these reactances linearly scale to the 15 000 rpm speed and results in the per unit values shown in Table 4. Of particular note is that a transient reactance is listed. This is somewhat contrary to Klontz's claims of PM machines having no transient reactance. From Klontz's discussion, it could be inferred that the transient reactance listed may actually be the synchronous reactance. Assuming that is the case, it follows with Klontz's discussion that PM machines tend to have much lower reactances than traditional wound-field generators. The low reactances make the machine more susceptible to demagnetiziation as compared to Sun's fault tolerate machine. However, the large magnetic gap (i.e., air gap and magnet and containment sleeve) and the very stable samarium-cobalt magnets protected this machine under terminal short-circuit conditions.

Table 4: Reactances of Bailey PM machine [22]

| AS TESTED PARAMETERS IN PER UNIT, $X_d$' AND $X_d$" | |
|---|---|
| | **Prototype** |
| $X_d$' [pu] | 0.525 |
| $X_d$" [pu] | 0.453 |

The greatest importance of the work by Saban and Bailey is that they have shown that a PM machine can be built to operate at multi-megawatt levels and turbine generator speeds successfully while being resistant to demagnetization. Part of this resilience comes from the mechanical requirements due to the significant weight of the rotor spinning at high speed. Also, a conservative approach to forces, thermal, and electrical parameters provided margin from initial design to measured results as is good engineering practice.

### 6.4 Machine Testing Relating to IEEE Std 115

In a paper by Saban, Gonzalez-Lopez, and Bailey, they discuss several aspects of the IEEE Std 115 [15], which pertains to acceptance testing of synchronous generators and motors, and where it is deficient in handling PM machines [23]. Many of the tests related to the stator can be conducted normally. However, since a PM machine has no field winding and non-adjustable field, some tests have to be altered.

As mentioned earlier, PM machines have no transient reactance though an equivalent can be determined. As such, short-circuit testing results must be interpreted differently. Separate-drive no-load testing would typically produce saturation curves between armature voltage and field current. However, since the field "current" is fixed, only one point can be obtained as shown in Figure 16. The curves of Figure 16 are example curves from the IEEE standard 115 standard with some additions by Saban. Point A indicates where the open-circuit curve would intersect the 1 per unit field

"current" line of a PM machine. Point B is on the Zero-PF-Rated-Current-Saturation curve. This test is done in an over-excited state which is not possible with the PM machine. Point C shows the more representative short-circuit point for a PM machine which tends to be above rated current.

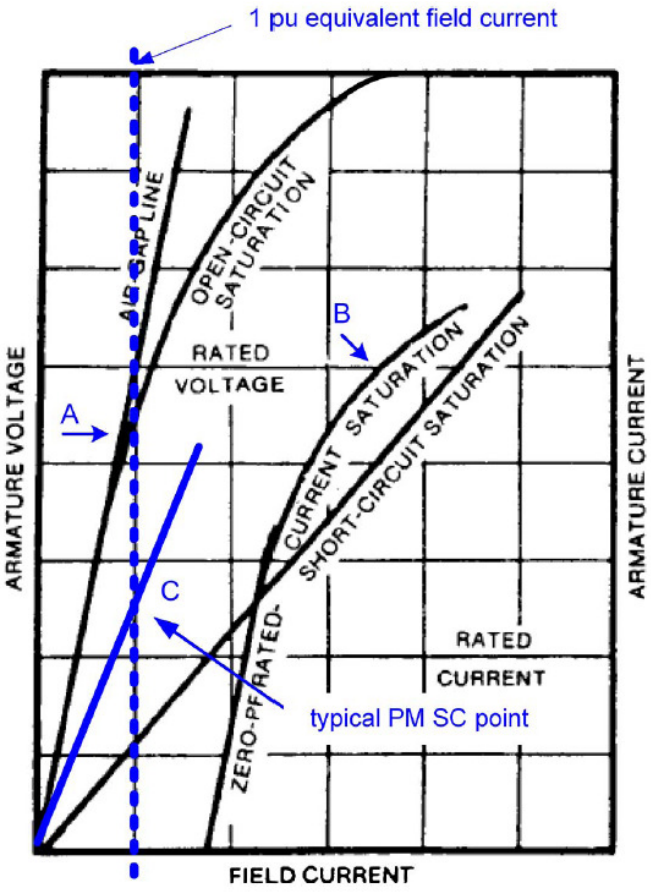


Figure 16: Saturation Curves from IEEE std 115 with modifications by Saban [23]

The torque tests in IEEE Std 115 are particularly problematic as the field can be neither open or short circuited as described in the procedure. However, these tests are mostly geared towards line started machines. As PM machines would typically be controlled by an adjustable speed drive, the starting behavior would be heavily influenced

by the control algorithms. Saban describes how to determine other machine parameters and segregate losses according to the test procedures, but he also mentioned how tests considerations must be made for demagnetization and magnet containment which are not needed for wound-field machines. It is also pointed out that for design qualification some of the tests must be agreed upon between the manufactures of a machine and the purchaser beforehand as there is some danger to the machine. This is especially the case in short-circuit and demagnetization testing where there could be some performance loss.

# Chapter 7

# Conclusion

In this report, several aspects of designing and operating high-speed high-power PM machines have been presented. The permanent magnet materials themselves are at the heart of the machine. Of the high quality materials, neodymium produces the highest magnetic field strength. However, samarium cobalt is much more thermally stable for only a small reduction in field strength. Numerous topologies are possible including surface mounted magnets, embedded magnets, and even interior placed magnets. In small machines, interior rectangular shaped magnets can be used to create salient machines. As the machine power increases, more iron is needed in both the rotor and stator to carry the magnetic flux. The large spinning rotor precludes some designs due to mechanical strength limitations. The high rotor surface speeds may exceed the tensile strength causing catastrophic failure. This generally leads to designs with solid rotor cores, magnets retained by adhesives or brackets, and possible retaining sleeves or cans covered the outside. Arkkio provides a rule of thumb to limit surface speeds to less than 250 m/s.

Due to its construction, a PM machine has no defined transient reactance. When doing short-circuit analysis, the transient reactance can be set equal to the synchronous reactance as done by Klontz [11] or a value can be determined experimentally as done by Saban and Bailey [22]. Both produce acceptable results to describe the behavior. PM machines tend to have lower reactances than their wound-field counter parts. This will lead to higher short-circuit currents which must be account for in the design. Unique to the PM machines is the potential for demagnetizing the permanent magnets result in permanent damage and reduced performance. Retaining cans or sleeves will make the air gap larger than required from an electromagnetic perspective. While this may lower the

potential output voltage, it provides added protection to the magnets in the event of a short-circuit.

Saban and Bailey showed that a PM machine can be successfully built and tested in the multi-megawatt operating at 15 000 rpm. The relatively simple rotor design is likely to provide similar reliability benefits as the squirrel cage or solid rotor did for induction motors. However, the lossy nature of the solid rotor induction machine which has poor power factor is avoided. Saban and Bailey's work showed that direct coupling to a gas-turbine was possible. This type of system could be attractive to several industries in addition to the petrochemical industry. There is significant push for naval ships to become increasingly electric. As such, high-speed high-power permanent machines could be useful in various roles for power generation, propulsion, and energy storage.

# References


[1] J. R. Hendershot, Jr., T. J. E. Miller, *Design of Permanent-Magnet Brushless Motors*, 1st ed. Hillsboro, OH: Magna Physics Publishing, 1994.

[2] R. Krishnan, *Permanent Magnet Synchronous and Brushless DC Motor Drives*, 1st ed. Boco Raton, FL: CRC Press, 2010.

[3] P. C. Sen, *Principles of Electric Machines and Power Electronics*, 2nd ed. John Wiley & Sons, Inc., 1997.

[4] R. H. Park, "Two reaction theory of synchronous machines generalized method of analysis – Part I," *Trans. AIEE*, vol. 48, no. 3, pp. 716-727, Jul. 1929

[5] T. Sebastian and G. Slemon, "Transient torque and short circuit capabilities of variable speed permanent magnet motors," *IEEE Trans. Magn.,* vol. MAG-23, no. 5, pp. 3619-3621, Sep. 1987.

[6] S. Morimoto, Y. Takeda, T. Hirasa, and K. Taniguchi, "Expansion of operating limits for permanent magnet motor by current vector control considering inverter capacity," *IEEE Trans. Ind. Appl.,* vol. 26, no. 5, pp. 866-871, Sep./Oct. 1990.

[7] J. Wang, K. Atallah, and D. Howe, "Optimal torque control of fault-tolerant permanent magnet brushless machines," *IEEE Trans. Magn.,* vol. 39, no. 5, pp. 2962-2964, Sep. 2003.

[8] Z. Sun, J. Wang, G. W. Jewell, and D. Howe, "Enhanced optimal torque control of fault-tolerant PM machine under flux-weakening operation," *IEEE Trans. Ind. Electron.,* vol. 57, no. 1, pp. 344-353, Jan. 2010.

[9] B. Stumberger, A. Hamler, M. Trlep, and M. Jesenik, "Analysis of interior permanent magnet synchronous motor designed for flux weakening operation," *IEEE Trans. Magn.,* vol. 37, no. 5, pp. 3644-3647, Sep. 2001.

[10] R. Dutta, and M. F. Rahman, "Design and analysis of an interior permanent magnet (IPM) machine with very wide constant power operation range," *IEEE Trans. Energy Conv.,* vol. 23, no. 1, pp. 25-33, Mar. 2008.

[11] K. W. Klontz, T. J. E. Miller, M. I. McGilp, H. Karmaker, and P. Zhong, "Short-circuit analysis of permanent-magnet generators," *IEEE Trans. Ind. Appl.,* vol. 47, no. 4, pp. 1670-1680, Jul./Aug. 2011.

[12] C. Concordia, *Synchronous Machines, Theory and Performance.* New York: Wiley 1951.

[13] B. Adkins, *The General Theory of Electrical Machines.* London, U.K.: Chapman & Hall, 1964.

[14] J. D. Glover, M . S. Sarma, and T. J. Overbye, *Power System Analysis and Design*. 5th ed. Stamford, CT: Cengage Learning, 2012.

[15] *Test Procedures for Synchronous Machines,* IEEE Standard 115, 1994.

[16] E. W. Kimbark, *Power System Stability.* Piscataway, NJ: IEEE Press, 1995.

[17] Z. Sun, J. Wang, D. Howe, and G. Jewell, "Analytical Prediction of the short-circuit current in fault-tolerant permanent-magnet machines," *IEEE Trans. Ind Electron.,* vol. 55, no. 12, pp. 4210-4217, Dec. 2008.

[18] F. D. Fielder and E. Beck, "Effects of lightning voltages on rotating machines and methods of protecting against them," *Trans. AIEE,* vol. 49, no. 4, pp. 1577-1586, Oct. 1930.

[19] A. Arkkio, T. Jokinen, and E. Lantto, "Induction and permanent-magnet synchronous machines for high-speed applications," in *Proc. 8th ICEMS,* Sep. 27-29, 2005, vol. 2, pp. 871-876.

[20] B. M. Wood, C. L. Olsen, G. D. Hartzo, J. C. Rama, and R. R. Szenasi, "Development of an 11000-r/min 3500-hp induction motor and adjustable-speed drive for refinery service," *IEEE Trans. Ind. Appl.,* vol. 33, no. 3, pp. 815-825, May/Jun. 1997.

[21] C. Bailey, D. M. Saban, and P. Guedes-Pinto, "Design of high-speed direct-connected permanent-magnet motors and generators for the petrochemical industry," *IEEE Trans. Ind. Appl.,* vol. 45, no. 3, pp. 1159-1165, May/Jun. 2009.

[22] D. M. Saban, C. Bailey, D. Gonzalez-Lopez, and L. Luca, "Experimental evaluation of a high-speed permanent-magnet machine," in *Proc. 55th IEEE PCIC,* Sep. 22-24, 2008, pp. 1-9.

[23] D. M. Saban, D. A. Gonzalez-Lopez, and C. Bailey, "Beyond IEEE Std 115 and API 546: test procedures for high-speed multimegawatt permanent-magnet synchronous machines," *IEEE Trans. Ind. Appl.*, vol. 46, no. 5, pp. 1769-1777, Sep./Oct. 2010.

# Vita

John Paul Bergstrom was born in Anderson, IN. He received his Bachelor of Science in Electrical Engineering from Rose-Hulman Institute of Technology in Terre Haute, IN in 2005. Mr. Bergstrom was employed by Bose Corporation from 2005-2009 in Framingham, MA. Mr. Bergstrom has been employed by Raytheon Company in Sudbury, MA since 2009 and has attended The University of Texas at Austin with sponsorship by Raytheon Company.

Permanent email: jpbergstrom@gmail.com

This report was typed by the author.